WORLDWIDE FIRST FULLY UP-SCALED FABRICATION OF 60 CM X 100 CM DYE SOLAR MODULE PROTOTYPES

A. Hinsch[1*], W. Veurman[1] , H. Brandt[1], R. Loayza Aguirre[1] , K. Bialecka[1] , K. Flarup Jensen[1]
[1]Fraunhofer ISE, Heidenhofstraße 2, 79110 Freiburg, Germany,
Correspondence to: hinsch@ise.fhg.de

ABSTRACT: Large scale (6000 cm^2) dye solar cell (DSC) modules were developed using the meander and integrated series connection design in combination with the glass frit sealing technique [1]. The manufacturing process, as developed at Fraunhofer ISE for glass frit-sealed DSC modules, is based entirely on screen printing and does not require the interconnection of sub-modules. With the same technique and appropriate quality control, a good reproducibility on smaller scaled modules (10 x 10 cm²) is already achieved and a solar efficiency of 7.1% on the active area has been reached, resulting in 5.3% efficiency on total aperture area. The scope of the recent work is to prove that the manufacturing concept is up-scalable to attractive areas for the BIPV market. To reach the size of 60 x 100 cm² it was necessary to transfer each process step into an industrial environment. Additionally a half-automated station for coloring and electrolyte-filling made out of standard parts was constructed which forms the basis for the final processing steps. Additional functions (processes and quality control) to ensure the long-term stability are integrated into the station. First operating module prototypes have been manufactured with this equipment. Different processing steps and the electrical characterization of these first 60 x 100 cm^2 prototypes are presented along with an overview of the advantages of this module concept in terms of cost effective up-scaling and transfer to industrial production.

Keywords: dye sensitized solar cell, module prototypes, up-scaling

1 INTRODUCTION

The dye solar cell (DSC) is a rather young technology that represents a completely new type of photovoltaic (PV) application. The production processes for this new technology are now starting to leave the laboratory and become mature, meeting industry standards for reproducibility through development towards up-scaling and quality control. As an important step in this direction, we have succeeded in producing the worldwide first large scale DSC module on a continuous substrate with dimensions of 60 x 100 cm^2 (see figure 1).

Figure 1: Prototype of a working 60 cm x 100 cm dye solar cell module manufactured at Fraunhofer ISE by fusing of two screen printed glass substrates. The module is internally 12-fold electrically interconnected in series. The module is transparent because the active layer is build-up of nano-particles with low degree of light scattering.

1.1 DSC principles and efficiency

Dye solar cells are photoelectrochemical solar cells. Their photon-energy-to-charge-conversion process is similar to the primary step in photosynthesis. The DSC technology presents a prime example for the research behind and the realization of functionalizing nanomaterials. Currently, world record calibrated efficiencies of 11.2 % and 10.4 % on active area are reported for small scale (0.3 and 1 cm^2) DSC and 9.2 % for a small DSC module (17 cm^2) [2,3]. At Fraunhofer ISE, a solar efficiency of 7.1% has been reached on 10 x 10 cm^2 DSC modules, where the active area constitutes 75% of total module area. The general setup of the cells is shown in figure 2a. The cells are based on a thin nano-crystalline carrier layer made of porous titanium dioxide (TiO_2) whose large inner surface area is chemically bonded with dye molecules. After photoexcitation of the dye molecules, electrons are injected and collected in the TiO_2 photoelectrode. A liquid redox electrolyte is used for transporting the remaining positive charge carriers to the counter electrode where the back-reaction takes place. The charge transport in DSC, i.e. electrons in the TiO_2 and electronic holes in the electrolyte is mainly limited by thermal diffusion, which explains the positive temperature behaviour in the solar efficiency of a DSC [3]. The charge recombination, which limits the photovoltage, predominantly takes place at the interface of the TiO_2 surface with the electrolyte. In the commonly used liquid redox electrolytes, triiodide (I_3^-) is the species which carries the electronic hole. This has strong implications on the performance and the long-term stability of DSC. At light intensities (0.1 to 1 sun), which are relevant for outdoor operation of a DSC, the photocurrent can only by transported through the electrolyte without loss, if the electrolyte has been made conductive enough by enhancing the “dark” triiodide concentration, which in reverse enhances the unintended electron recombination. Also, for a stable long-term operation of a DSC, a permanent consumption of triiodide through non-regenerative side reactions with e.g. electrolyte impurities has carefully to be omitted [4, 5]. The optimization of the cell efficiency requires a well thought balancing of the gain and loss factors in the system [6]. In the past, several strategies have therefore been followed with the aim to enhance the efficiency of DSC further [7].

Since the DSC contains a liquid, oxidative electrolyte, a good sealing method is crucial to both

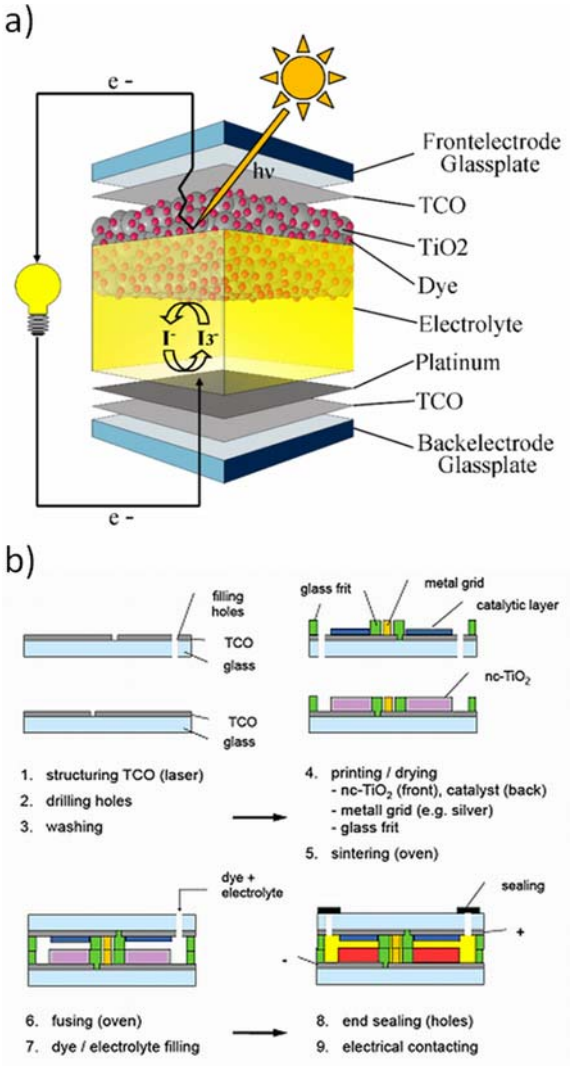

Figure 2: a) Working principle and device structure of a dye solar cell. A redox active organic electrolyte transports the positive charge between the porous photoelectrode and the counter electrode. If transparent substrates are used, then the DSC is photoactive from both sides. b) Manufacturing scheme for dye solar cell modules as developed at Fraunhofer ISE. The cross section at the electrical interconnect is shown.

protect the metal current collectors and to prevent leaking of the electrolyte. For the modules described in this article, a low melting glass in the form of a glass frit is used. The glass frit can be screen printed and forms a very tight seal.

1.2 New design possibilities for building integrated PV

Being a glass element that also generates electrical power, the DSC technology is ideal for building integrated photovoltaics (BIPV) [8] as shown in figure 3a and b. The modules are printed on glass and therefore uniquely offer a high degree of freedom for the design and the aesthetical appearance. The many options can be grouped in the following categories:

Transparency: when using well dispersed TiO_2 nano-particles with a size between 10 - 20 nm, the visible light will hardly be scattered by these particles and so, the modules will appear transparent. By introducing larger TiO_2 particles (>200 nm) into the layer, the light scattering can be gradually increased, until the point where the modules will be 100% opaque. As a result, by printing light scattering coatings onto the photoelectrode within the module, any arbitrary images and logo type text can be created with a negligible loss in electrical power output as is shown in figure 3c.

Active area color: The module prototypes are of amber color but other colors are also possible. The color of the active area is a result of the dye in combination with the yellow color of the electrolyte, caused by the triiodide. When the active layer is thicker, more dye will be adsorbed, which results in a higher optical influence on the collor of the dye in regard to the influence of the electrolyte. In our modules to date, using a standard ruthenium based metal-organic dye, a thicker active layer would result in an increasingly intense red-amber appearance instead of amber. This can nicely be seen in figure 3c where both colors are shown. The standard dye has a red color, but newly developed pure organic dyes [9] of different color will also be tested and applied in the modules in the future.

Glass frit encapsulation color: The use of colored glass frit pastes can either highlight the pattern of the module, or give it a much more homogeneous appearance.

Form and shape: So far, square shaped modules were built, but other shapes or bended structures can be achieved as well.

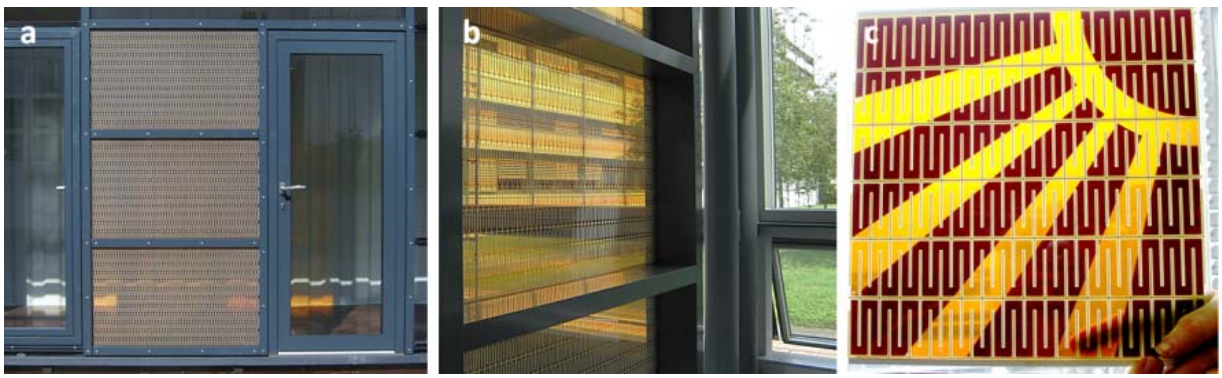

Figure 3: Photos a) and b) demonstration of real DSC BIPV façade applications made by Fraunhofer ISE; photo c) example of design freedom in a "deco-type" DSC application: a scattering layer is applied in the cell interior, this way, images and logo type text can be created with a negligible loss in electrical power output.

Application of foils: with a light filtering top or backside foil the color in transmission or reflection can be neutralized to grey or black or can be enhanced respectively. Another way to alter the optical appearance of the module in front view can be realized by applying a metallic foil or a metal like reflecting layer onto the backside glass.

1.3 Low-cost production

The basic manufacturing of a DSC is very simple. The modules are produced by screen-printing and do not require expensive vacuum technology. Therefore, DSC production is regarded as a potentially low-cost technology. The required amount of active material per area is low; less than 1 g/m^2 for the dye, approximately 15 g/m^2 for the TiO_2 and less than 30 ml/m^2 for the electrolyte. In fact, from cost estimations conducted by Fraunhofer ISE and other project partners [10], it is estimated that the main material cost contribution comes from the glass substrates. As substrates, low-cost flat glasses are used that are coated with a transparent conductive oxide (TCO, fluorine doped tin oxide).

In parallel to the technology and the module development, cooperation with leading architects from the field of BIPV was set up. For that purpose expert interviews and workshops were conducted to evaluate the requirements for DSC modules in several applications of BIPV. Wall cladding, structural glazing and rooflights were the three scenarios regarded in these studies. An important outcome of the workshops was that applications of DSC based BIPV will be financially competitive with standard non-PV façades, when the substituted façade material and the return of energy by the PV modules are taken into account. From the investigation an additional 100 €/m^2 can be estimated as the tolerable cost contribution of a DSC module to the sales price of a glass façade element.

1.4 LCA and energy payback time

In a recent European project “Robust-DSC”, a life cycle analysis (LCA) has been carried out for glass based DSC modules of Fraunhofer ISE [10, 11]. The LCA is a tool for analyzing the ecological impact of new products, materials and production processes. It is shown, that more than 70% of the impact on the indicators human health, ecosystem quality and resources depletion are originating from the glass substrates alone. The additional contribution of the DSC specific materials and processes is therefore low and does not represent a high initial load in the LCA balance. This is also true for the energy payback time, which for a south-oriented DSC façade is determined to be 0.5 to 1.5 years depending on the geographic location and the assumed module efficiency (5 – 7 %). In other words, if a DSC module is integrated into a glass façade which spares at least one glass substrate, the energy which is associated with the production and construction of the façade can be returned back at a good ecological value during the lifetime.

1.5 Recycling

In addition to the LCA, an important point for evaluating a new solar technology is the ability to recycle the modules. As the main part by volume (> 99%) of a DSC module consists of pure glass, the recovery of the glass in the necessary purity is crucial. A comparable case can be seen in the recycling from automotive rear window glass. As a side effect the recovery of the precious metals, in the priority order of silver (< 7 g/m^2), ruthenium (< 0.1 g/m^2) and platinum (< 0.05 g/m^2), as well as of iodide (< 5 g/m^2) is preferable. In the following, one example for a recycling procedure is given which is based on preliminary experiments we have conducted for this purpose. The module is mechanically disintegrated and the volatile components of the electrolyte, if any, are recovered by vacuum distillation, then the pieces are washed in an alkaline detergent solution to dissolve the dye ruthenium metal complex, the TiO_2 layer and the remaining iodide containing electrolyte components. Through further grinding of the glass pieces in combination with an acid treatment, the remaining DSC components can be separated from the glass by sedimentation.

1.6 Manufacturing and automation

The current manufacturing of the DSC modules at Fraunhofer ISE follows a nine step approach as is illustrated in figure 2b. The first three preparatory steps for the glass substrates include hole drilling, laser-structuring for electrical insulation of adjacent cells on the TCO, and washing. The next, most important production step is the screen printing (figure 4b).

Figure 4: a) Photo of an automated pilot-type equipment which has been developed at Fraunhofer ISE for the dye and electrolyte filling as well as for the final sealing of the large area dye solar cell modules, b) high precision screen printing of the TiO_2 photoelectrode layer onto the TCO-glass substrate for a large area dye solar module as developed at Fraunhofer ISE.

All layers including the encapsulating glass frit paste are screen printed and then dried. The organic residues of the printed layers are subsequently removed by simple sintering. Then, the plates are positioned and fused in an oven without applying mechanical pressure at temperatures which allow the glass frit to join and to form a tight external and internal seal. During the fusing process, the mechanical stress in the glass is released and the plates are self settling at a constant distance of approximately 50 microns, which in the ideal case results in mechanical properties comparable to a single glass

pane. As a result, a prefabricated module is obtained in which the active materials are well protected from surface contamination during further handling. In the final steps, dye solution and electrolyte are purged through the filling holes which are sealed afterwards. The advantage of the filling method is that the high quality chemicals can easily and safely be handled in small amounts per module in a closed tube system. This is essential for the long-term stability as the unwanted uptake of oxygen and water vapor in the module is prevented.

A further reduction of the process steps by means of process integration can be imagined which will decrease costs as well as energy demand even more and will enhance the throughput speed and the reproducibility. In an ideal production scenario which is shortly sketched here, the TCO coated glass substrates which are running off the float-glass line are directly cut, drilled and structured by laser which is avoiding contamination and therefore the critical washing step. Then printing of the layers will be performed in-line using a large area integrated screen-printer/dryer manufacturing line. Optionally, a combination with other well established wet coating methods like curtain coating or ceramic ink-jet printing is imaginable. Such glass printing lines are known to be capable of handling several to more than 10 square meters of glass substrates per minute. For the tempering steps sintering and fusing, a combined energy saving solution can be assumed, which makes use of in-line or larger batch type furnaces which are equipped with a suitable positioning and handling system. With the aim to save further thermal process energy, even a major part of the heat which is released from the cooling section of the float glass line might be utilized for this purpose. The machines which are necessary for the process steps of dye and electrolyte filling are by principle identical and are very well adapted to parallel processing as no process parameters have to be changed during the process time. Based on the results achieved with our pilot-type equipment, a process time for coloration in the order of 10 minutes per one module can be derived, if a highly concentrated (> 10 mMol/l) dye solution is applied. Machine units which can handle 10 – 30 modules per unit are easily conceivable. The automation of the filling hole closure process could e.g. be done with state-of-the-art pick and place equipment and by employing either UV LED spots for curing or e.g. laser sources for melting of the sealing material.

Most of the specific processes which are used in manufacturing of DSC modules are already well known in industry. As soon as pilot-line fabricated modules have been developed to a stage where a BIPV module certification has been achieved, an automated production line with high throughputs can be realized in a short time frame. The usage of a printed glass frit in a high volume production is a well known technique and has in particular been established for the production of large area plasma displays; although for the latter, the demands on accuracy are even higher. Interestingly, the glass substrate, the glass handling and the thermal treatments are similar to the ones which are already well established in the cost-effective production of thin film solar modules; although substantial lower investment costs can be assumed for DSC, as no high vacuum equipment will be necessary.

1.7 The DSC challenge

DSC's have been under intensive investigation as a new type of solar cell technology for over 15 years. In contrast to earlier expectations, the transfer from the laboratory stage to a module production phase has turned out to be time demanding. The challenge in the development of marketable DSC products is to maintain the idea of the simple basic manufacturing principle and to transfer this advantage into the up-scaling phase. The main hurdle for these cells has been their long-term stability. In the last few years though, more and more research groups world-wide have been able to show good stability results for these cells in accelerated ageing tests similar to standard photovoltaic module certification, i.e. 1000 hours at 85 ^{o}C, 1000 hours illumination at 1 sun and -40 ^{o}C to 85 ^{o}C thermal cycling [12-15].

We believe that a low water and oxygen content in the cells is the most important factor that contributes to their stability. To decrease the amount of oxygen and water diffusion into the cells a tight sealing material is necessary. The liquid and oxidative electrolyte forms an extra complication for the encapsulation. The electrolyte has a higher thermal expansion coefficient than the surrounding glass and besides tends to react with the silver current collectors. Also, the diffusion of electrolyte species through the serial interconnect has to be avoided to prevent electrophoresis effects during long-term operation [16]. The durability and accuracy of the encapsulation is therefore of utmost importance for DSC modules. As a consequence, module stability goes hand in hand with reproducible production standards and quality control.

1.8 New developments

The scope of the recent work at Fraunhofer ISE was to prove that the manufacturing concept is up-scalable to attractive areas for the BIPV market. To reach the size of 60 x 100 cm² it was necessary to transfer each process into an industrial environment. For applying the dye and the electrolyte, a half-automated station for coloring and electrolyte-filling made of standard parts was constructed which forms the basis for the final processing steps. Additional functions (processes and quality control) to ensure the long-term stability are integrated in the station. In this paper we will comment in detail on the manufacturing concept of the modules and their different processing steps. The electrical characterization of the first 60 x 100 cm^2 prototype will be presented along with a comparison to results on small 10 x 10 cm^2 modules and results of their stability.

2 EXPERIMENTAL

2.1 Meander type module design

All prototype modules were developed using the meander design concept. Figure 5 shows the CAD-design of the small scale 10 x 10 cm^2 modules. The module consists of two internally serial connected cells. Through the screen-printing of current collectors and glass frit an internal serial connection is automatically incorporated. To save material costs the front and back electrode are contacted over small so-called "Z-contact" points. These are shown in more detail in the lower inset of figure 5.

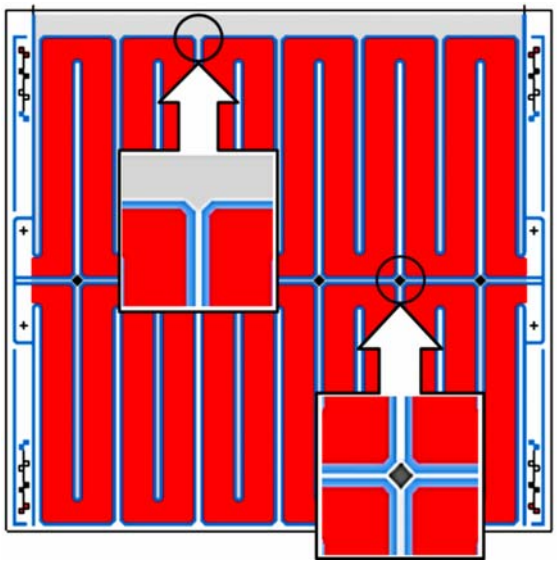

Figure 5: CAD drawing of the front electrode for the small scale 10 x 10 cm^2 modules. The red color represents the active area of the cells, blue shows where the glass frit is deposited, light grey stands for the silver current collectors, dark grey shows the internal electrical interconnection between adjacent cells. The upper inset shows the outer contact which penetrates into the cell via fork-like structures, the lower inset show the interconnection in more detail.

In the meander design the area of each single cell is increased by forming snake-like bends or a so called meander of glass seal around the silver contact lines. The meander type module concept was developed to have an optimal protection of the metal conductors. Also, the diffusion of electrolyte ions through the TCO layer underneath the glass seal between adjacent interconnected cells is blocked efficiently, as the TCO is removed on both sides.

Another advantage of this design lies in the reduction of the number of filling holes. Every single cell needs its own two filling holes to purge the colouring solution and the electrolyte through. These holes need to be sealed after the filling process, which is a complex, costly and time-consuming process. For the DSC technology, a stripe design would in principle just a well be possible; but an equivalent stripe design module with an area of 10 x 10 cm^2 would need 24 holes, in order to maintain the optimal cell width, in this case 8.5 mm [16], instead of 4 in the case of the meander design. For the larger 6000 cm^2 modules, which in principle uses the same design, the meander design needs 24 holes, whereas a stripe design would need no less then 150 holes.

For the 6000 cm^2 modules twelve solar cells are internally connected in series. The design for the larger modules is in principle the same, though a broader glass frit line is applied in the larger modules; 1.25 – 1.5 mm instead of 0.5 mm in the smaller modules. This low-risk option was chosen for the large scale prototypes to reduce the risk for failures in the encapsulation, which might be introduced by dust during the handling and transportation. The disadvantage is that the active area is reduced to 50% in the larger modules instead of 75% in the small scale modules. As soon as the glass handling and screen-printing for the larger modules is more automated in the future, the active area can easily be increased to 75% as well.

2.2 Module production process

The manufacture of the 60 x 100 cm^2 module prototypes at Fraunhofer ISE is carried out using industry-relevant procedures and machines. The same basic manufacturing procedure is used for the small 10 x 10 cm^2 modules. As substrates 3.2 mm float glass coated with fluorine doped tin oxide (FTO) is used (TEC-8, Pilkington) for the front as well as for the back electrode. The glass substrates are mechanically cut to the right size and the filling holes (at the back electrode substrates) are drilled either by laser or water-jet in the same run. Then a special type of laser is used to structure the TCO layer on the glass in order to electrically insulate the adjacent cells. This high energy, short pulsed laser is used in order to avoid the formation of micro-cracks in the glass. Standard Nd:YAG lasers fail in this case. After these laser preparation steps, the substrates are washed mechanically using demineralized water. The small modules are additionally treated by ultrasonification and rinsed with isopropyl alcohol.

Then all the layers, including the glass frit sealant and the ultra thin platinum back electrode layer, are screen printed. Between every print, the layers are dried using hot circulating air and negative pressure. The glass frit sealant is a lead- and bismuth free paste which is based on a $ZnO\text{-}SiO_2\text{-}Al_2O_3$ composition. For the catalytic back electrode a nano-colloidal platinum paste is used (3D-nano / Poland). Furthermore, for the TiO_2 layer and the silver contacts commercially available pastes were purchased (Dyesol DSL 18 NR-T, Ferro lead free silver paste). To burn out the organics from the printed pastes, the front and back electrodes are then sintered in an oven. The resulting active layer thickness of the TiO_2 is 2.5 µm for the large module prototype. The small modules were produced using varying thicknesses for the active layer between 2.5 µm and 7 µm. After the sintering step, the front and back electrodes are carefully positioned on top of each other and sealed tightly in a second furnace step. For both steps common glass fusing ovens were used (KSO-Gobi), heating the substrates by IR rays from the top and using a thin graphite foil as an under layer. To reach the necessary quality of the glass frit sealing, sinter- and fusing curves were developed which are passing the melting point of the glass particles very carefully. Heating up and cooling down in the fusing step has also to be done carefully to prevent bending of the TCO glass substrates.

When the oven steps are completed, the modules are colored through the filling holes (diameter 1 mm) at the back electrodes. For the large modules a pure solution of 0.3 mM N719 dye in ethanol was used. After coloring, the modules were dried by purging nitrogen.

For the small modules, a pure solution of 0.3 mM C101 dye in e.g. di-methylsulfoxide (DMSO) was applied. The C101 dye is a newly developed dye with a slightly higher absorption coefficient [17]. Since this dye is a new development, the production volume is still low and therefore this dye could not yet be applied for the larger modules. After coloring, the small modules were rinsed with acetonitrile (ACN) to wash out the DMSO and then dried with purged nitrogen.

After coloring and drying, the modules are filled with electrolyte immediately. For the larger modules a low-volatile electrolyte was applied which contained: 0.1 M Iodine, 0.1 M Guanidiniumthiocyanate (GSCN), 0.5 M n-butylbenzimidazole (NBB) dissolved in the ionic liquid phenylmethylimidazole iodide (PMIM) with 10 w% ACN (Merck / Germany). For the small modules a commercial volatile electrolyte was used from the company Dyesol (Dyesol EL-HSE). After filling, the holes are cleaned and sealed with a small 0.3 mm thick glass plate and UV curing glue (Threebond).

2.3 Half automated coloring and filling equipment

For applying the dye and the electrolyte, a customized, in-house development was necessary. Therefore, in cooperation with the Fraunhofer IAO in Stuttgart, Fraunhofer ISE developed a station (figure 4a) for automatically filling and final sealing the large area dye solar cell modules. A precise control of the liquid flow and a method for leak detection in the seal is possible. For the leak detection a gas overpressure is applied fully or partially to the inner parts of the module and the pressure drop is monitored. With this apparatus, the further manufacture of modules for future demonstration projects and field testing is guaranteed, and a decisive step towards a pilot processing line has been accomplished. The equipment has been designed such, that standard components from automation (Festo GmbH) and for the handling of liquids (Bürkle GmbH) have been integrated. Chemical inert manifolds and tubing (inner diameter 0.8 mm) made from Teflon material are used. As a result, a very low dead volume is necessary. Specific rubber based sealing parts have been developed which provide a pressure tight seal to the filling hole openings. In the coloration process, the dye solution is pressed through the module by applying a constant gas pressure of 3 bar to the liquid and is transported back into the reservoir. For the drying process nitrogen gas is purged through at a similar pressure. The electrolyte is first degassed by ultrasonification and then pressed into the module with a syringe pump. For the sealing of the filling holes, the equipment is additionally fitted with an automated disperser for dispensing of a UV-curable glue, as well as a plasma cleaning torch and a high power UV-LED.

2.4 Measurement methods

For the small scale modules, photocurrent characteristics were measured using a type A solar simulator, set to 1000 W/m^2 equivalent intensity for the DSC. The slew rate was 80 mV/s during the measurement. The temperature was controlled by gluing the back electrode on a copper plate, using thermally conductive paste and measuring the temperature on the front glass.

The EIS measurements for the small scale modules were done using a sulphur lamp set-up, which had an intensity of ~800 W/m^2. The temperature during the measurement was controlled by a ventilator and measured to be 45ºC ± 2 ºC. The potentiostat (Electrochemical Workstations IM6 Zahner) was set to V_{oc} with a perturbation amplitude of 10 mV.

The large scale modules were measured outdoor on a sunny day on the roof of the Fraunhofer ISE (inset figure 6). The slew rate was 100 mV / s. The intensity was recorded using a pyranometer and the temperature was measured with a sensor at the back of the module to be 45 ºC ± 5 ºC. The maximum intensity recorded on that day was 821 W/m^2 due to diffuse clouds in the higher atmosphere.

3 RESULTS AND DISCUSSION

3.1 Electrical characteristics

Electrical calibration of DSC modules is challenging since standard equipment used for the calibration of conventional solar cells and modules is not one-to-one applicable. The main difference lies in the slow electrical response of the cells. In the DSC, the porous TiO_2 with its high internal area is used as a carrier material for the photoactive dye and as an electron transport medium. The porous network does not form a perfect crystal structure, but contains many isolated conduction band states, which act as long-living (> seconds to minutes) traps for the electrons. This high amount of trapped, negative charge in the TiO_2 is screened by the positive cations from the electrolyte and is the cause for the high capacitance of DSC cells and therefore their slow electrical response [18].

The transport of the electrons through the TiO_2 can not be regarded as band-transport but is considered as diffusive transport. When light is illuminated on the cell, a dynamic process takes place in which traps are filled and an electron concentration gradient is build-up which supports the diffusive transport. Depending on the electrolyte used, this process can take up to several milliseconds. When the external load is changed, the electron concentration gradient in the TiO_2 is changed via this relatively slow dynamic process. Therefore, when scanning the photocurrent characteristics for these cells, slew rates of <100 mV/s generally need to be used. Compared to conventional solar modules, where the electrical response can be measured with flashed light within milliseconds this is slow. Also, when measuring spectral response of the cells and modules, chopper frequencies and bias light illumination need to be adapted.

To circumvent these problems for the beginning, the large scale modules were measured outdoor using measurement equipment which can measure with 100 mV / s.

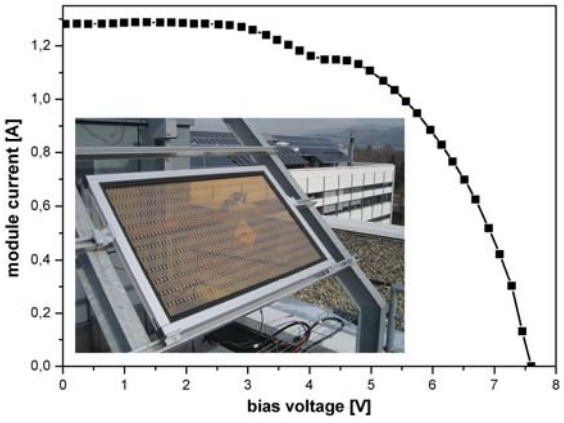

Figure 6: Photocurrent characteristics for first 6000 cm^2 DSC prototype module, measured outside on the roof of the Fraunhofer ISE. The “bump” at 3 to 4 Volts is caused

by the non-optimized frame, which partially shades the first and last cell in the module.

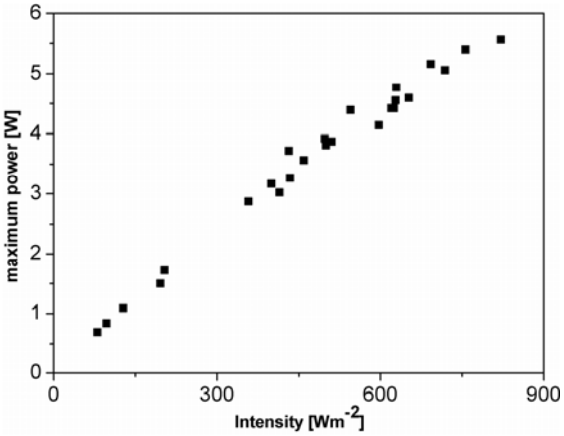

Figure 7: Intensity dependence of the maximum power produced by the large scale module in the outdoor measurement set-up.

Another complicating factor for the precise calibration is the temperature. DSC's are glass- glass sealed devices, which makes the control and precise measurement of the temperature during illumination more challenging. To reduce measurement time, the temperature was measured at the back of the modules (large modules) or as a gradient between the front and back electrode (small modules).

Figure 6 shows the photocurrent characteristics for the large scale module at 821 W/m^2. The module temperature during this measurement was 45ºC ± 5 ºC. In figure 7 the intensity dependence of the maximum power delivered by these modules can be seen. The intensity dependence is dominated by the current response which is linearly related to the light intensity.

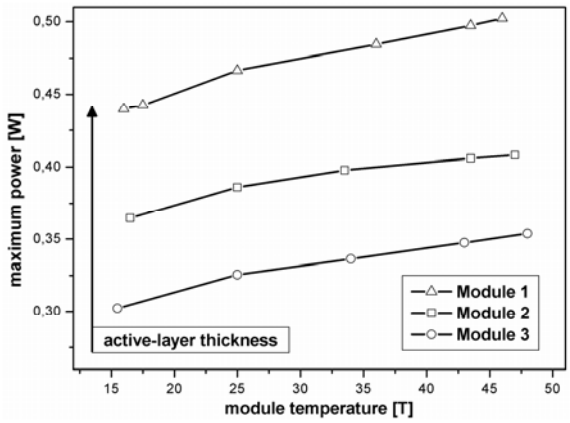

Figure 8: Temperature dependence of the maximum power produced by small scale modules, having active layer thicknesses between 2.5 and 7 µm, measured using a type-A solar simulator.

Figure 8 shows the maximum power at different temperatures for 100 cm^2 modules 1, 2 and 3 having transparent active layer thicknesses of 7 µm, 3.5 µm and 2.5 µm respectively. The active layer thickness of 2.5 µm of module 3 is the same as for the 6000 cm^2 modules. Modules 1 and 2 have thicker active layers, resulting in the color change of the modules from transparent yellow-amber to transparent red-amber. A typical feature of DSC modules is the positive temperature dependence, in contrast to other PV technologies, the efficiency increases with increasing temperature. This is mainly due to an improved fill factor (FF) at higher temperatures. Intrinsically, the FF depends on the dynamic properties of the cell for recombination and charge transport through the TiO_2. Since this is a diffusion transport, the temperature dependence is positive.

Module	P_{MPP} at 1 Sun	Active area	η A_{active}
6000 cm^2 (2,5 µm TiO_2)	6,5 W	48 %	2,3 %
100 cm^2 (2,5 µm TiO_2)	0,33 W	75 %	4,4 %
100 cm^2 (7 µm TiO_2)	0,46 W	75 %	6,1 %
100 cm^2 (14 µm TiO_2 /opaque)	0,52 W	75 %	7,1 %

Table 1: Comparison of module efficiencies on the active area for small and large scale modules and variation in active area thickness.

Table 1 shows the compared efficiencies on the active area for small and large scale modules, these efficiencies are not calibrated values. They are estimations since the temperature control was poor during these measurements. Still it can be easily deduced that the efficiency for the large scale module is low compared to the smaller modules, with only 2.3 % whereas module 3 has an efficiency of 4.4% on active area. One of the reasons is the use of a different dye and electrolyte, which shows nicely the relation between DSC cell performance and the used chemicals. Another reason for the lower efficiency is the bump which can be seen in the photocurrent response for the large module in figure 6. This is caused by partial shading of the module by its mechanical frame, which can be seen in the inset of figure 6. The frame was necessary to safely and securely fasten the module to the outdoor measurement construction set-up. This framework still needs to be optimized and at the moment it shades the first and the last cell by three millimeters. This is equivalent to about 10% of the active area of each of these cells. Due to the cell shading the FF is reduced slightly for the large module.

3.2 Stability testing

Figure 9 shows the results for stability test at 85°C in the dark at V_{oc} for a 100 cm^2 module. It can be seen in figure 9b that initially, the FF was very poor. But then, after the first 100 hours of accelerated aging, the FF is improved dramatically (black curve, initial IV curve; red curve, after 100 hours of aging). After the next 900 hours, this effect is not reversed anymore. This effect is seen consistently for our modules and is due to the improved functionality of the platinum back electrode during the temperature treatment, which will be further discussed in the next paragraph.

Another effect seen during the aging is the increase of the photocurrent in the first 100 hours. This is thought

to be due to the consumption of triiodide caused by photodegradation of organic material catalysed by the TiO_2 in the presence of water and or oxygen. The triiodide is important for the p-type charge transport in the cells, which is a diffusion transport. Therefore, the transport is improved when the concentration is higher. A drawback of a higher triiodide concentration is the increase in recombination processes with electrons from the TiO_2. Therefore there is an optimum for the triiodide concentration which forms a best possible balance between these two processes. For our cell system this concentration is between 30 mM and 50 mM. For the module the initial triiodide concentration was 100 mM in the electrolyte. Due to the small amount of water and oxygen initially present in the module in the electrolyte and on the surface of the TiO_2, this concentration is decreased during the aging and reaches the optimal concentration after about 100 hours. After 1000 hours the current has relaxed back to the original value. The water on the surface of the TiO_2 has a positive effect on the V_{oc} due occupation of surface states. After complete consumption of the water the V_{oc} relaxes back to a lower value.

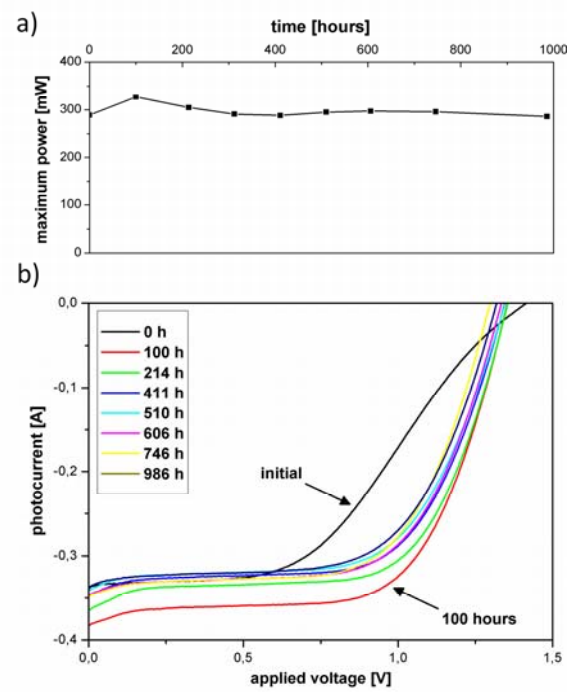

Figure 9: a) Stability test of 1000 hours at 85°C in the dark at open circuit for a 10 x 10 cm^2 module, the figure shows the MPP of the module during the stability test, b) photocurrent characteristics of the module during the stability test.

Figure 9a shows the power of the module at MPP, which is directly related to the efficiency of the module. The main cause for the degradation of the modules is the V_{oc} decrease during time; this is in part compensated by the initial increase in FF and $J_{sc;}$ therefore the overall loss in efficiency after the accelerated aging is less then 1%.
To test the mechanical stability of the modules under extreme circumstances, hail tests were performed both on the small and on the large scale modules. Special designed hail balls with a diameter of 2.5 cm were shot with a speed of 23 m/s on different spots on the module. The module did not have a frame, it was mechanically supported by four clams at the edges, it was not specially prepared or protected, apart from the normal front and back electrode glass substrates. Afterwards, the module did not show any damage, nor by visual inspection or with optical microscope. This shows the high durability of the glass-glass sealed modules. The hail test is an important standardized test when it comes to roof type applications.

3.3 Influence of temperature treatment on the functionality of the back electrode

Figure 10 shows the results of an EIS measurement under illumination of a typical 100 cm^2 module kept at V_{oc}. The black squared symbols in the graph show the initial measurement of the fresh module, just after filling and sealing. The interpretation of the spectrum was done using a one diode model equivalent circuit which was adapted for DSC [19]. The R_s is determined from the first part of the spectrum to be 0.44 Ω. The functionality of the platinum for catalyzing the back reaction or the so called charge transfer resistance can be determined from the first semicircle to be 7 Ωcm^2. The total resistance at V_{oc} was 1.2 Ω. The R_{ct} makes up about 1/4 of this value. It adds up to the total resistance of the module and therefore is lowering the FF. The high R_{ct} is thought to be caused by the coloring procedure which necessarily takes place after the fusing of the front and back electrode, due to the module design. Measurements on symmetrical cells with platinized TCO electrodes showed much better R_{ct} [20].

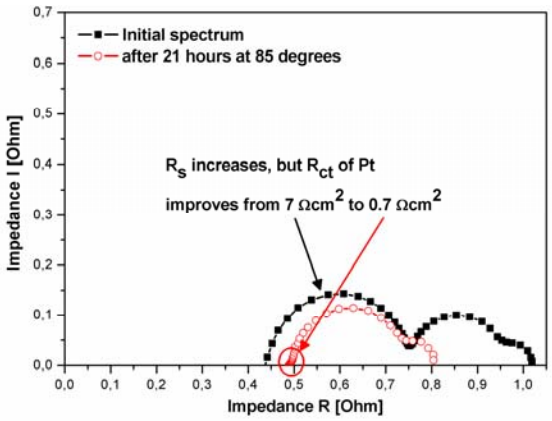

Figure 10: Electrical impedance spectrum of a fresh module and the same module after 21 hours at 85ºC.

It was observed that after less than a day of storing the module at 85°C, the R_{ct} decreased dramatically from 7 Ωcm^2 to 0.7 Ωcm^2 (red circle symbols in figure 10). The first semi-circle in the impedance spectrum can hardly be detected anymore; this shifts the other two semi-circles to the left in the spectrum, causing the total resistance around V_{oc} to be lowered, which in effect increases the FF of the module. At the same time the total series resistance is also increased slightly, which can be seen from the higher onset of the spectrum.

3.4 Photocurrent mapping

To investigate the function of the current collectors in the meander design, a small scale module was scanned by photocurrent mapping using a small red laser diode to

illuminate a 1mm intersection spot. The result for one meander is shown in figure 11. It can be seen that the current is homogeneously extracted from all parts of the meander.

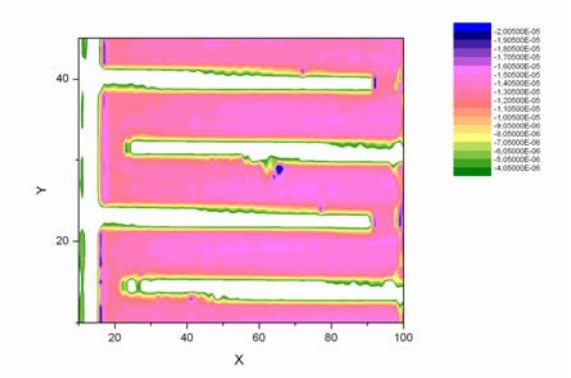

Figure 11: Photocurrent mapping of part of the meander design of a 100 cm^2 module, the photocurrent is shown as a negative current.

3.5 Quality control

A successful up-scaling and a future certification of DSC modules can only be realized when a good quality control of all the materials is carried out. Some processes and materials are indentified as more critical then others. Based on the experience achieved during prototype manufacturing of DSC modules at Fraunhofer ISE, the most critical materials are listed in Table 2.

Material	Process	Quality
TCO	cleaning	Contamination free
TCO	Laser structuring	Crack free
TiO_2 layer	Screen printing and drying	Homogeneous and crack free
Glass frit layer	Screen printing and drying	Homogeneous and wetting of TCO

Table 2: Critical module materials and processes which need improved quality control

The TCO glass commercially is fabricated in an atmospheric pressure chemical vapour deposition (APCVD) coating process directly inline with the manufacturing of float glass. Although the TCO glass is produced in large quantities, in particular for the manufacturing of thin film CdTe solar modules, the purchased glass is often heavily contaminated at the surface due to inappropriate handling (transportation and cutting). With scanning electron microscopy (SEM) we have been able to trace different types of contamination, both of organic and inorganic origin. Figure 12 shows different examples. Also pure mechanical scratches have been observed. In particular oil contaminations tend to be hazardous since they will spread over a large area forming a very thin film on the TCO. They can be seen by SEM in low magnification (figure 12c) mode, but they are not optically visible because of the rough TCO surface. They will have a bad effect on the TiO_2-TCO contact after sintering. Cleaning of the TCO glass with standard methods from the glass industry (rotating brushes and demineralised water) are believed to be insufficient. In the ideal case, the production of DSC modules would have to be combined with the TCO production, and contamination free glass cutting should be applied. The structuring of the TCO layer by laser is not only required for the electrical insulation of adjacent cells, but also has a barrier function. Microcracks in the glass are therefore not tolerable. With a standard Nd:YAG laser the immediate or delayed formation of microcracks could not totally be avoided in the TCO samples we tested. With an improved short pulsed, high energy laser technique, a crack-free, very selective removing of the TCO layer has been achieved (figure 13).

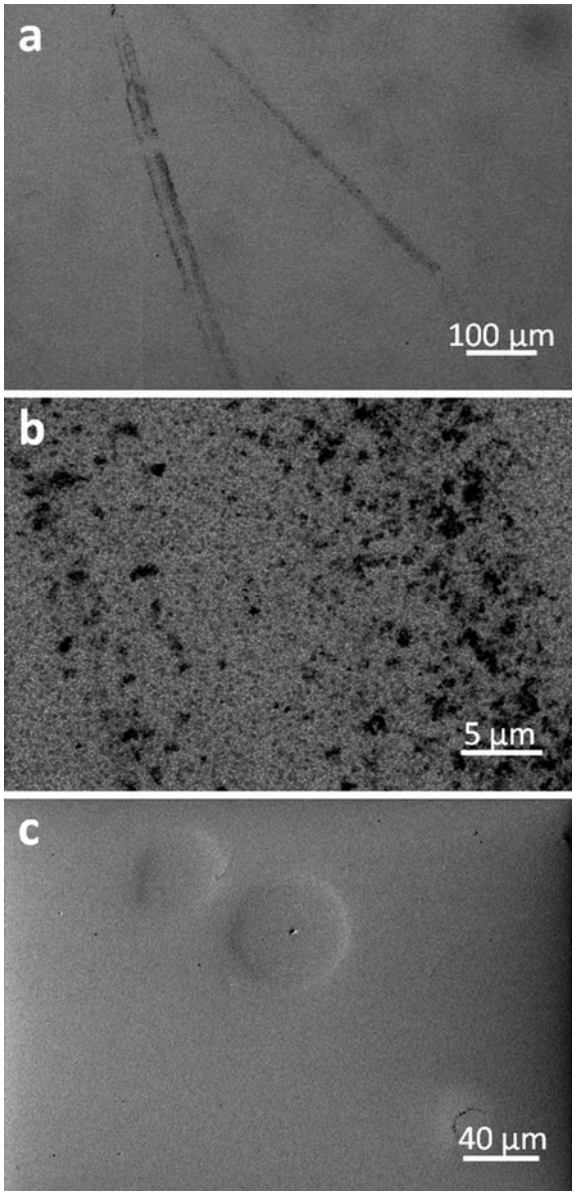

Figure 12: SEM images from contaminations on the TCO glass surface a) at low magnification, and b) at high magnification, c) SEM image at low magnification of TCO contamination with oil drops.

The quality of the TiO_2 layer is crucial for achieving a good solar efficiency of the dye solar module. The electron transport (diffusive or also called hopping transport) through the porous TiO_2 layer can be decreased by the recombination of electrons with the

electrolyte at the interface between the particles. Figure 14a shows the interface between the TiO_2 layer and the TCO. An insufficient contact between the TiO_2 nano-particles and the TCO layer could result in a loss of electrons by the same recombination process. A high disaggregation of the TiO_2 particles nearly down to the primary particle size (10 - 20 nm) in the screen print paste is necessary to avoid the presence of aggregates during the film formation. TiO_2 particles in these aggregates can not follow the roughness of the TCO crystals in the TCO layer which results in point contacts, i.e. partly insulated parts of the TiO_2 layer which are in the sub-micron range.

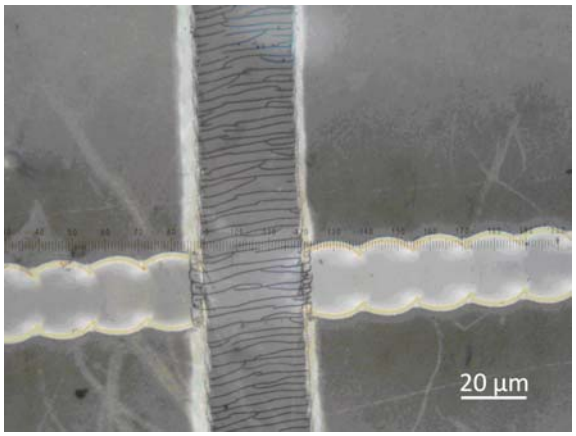

Figure 13: Microscopic image of laser structured TCO; standard Nd:Yag (vertical line), other laser (horizontal line).

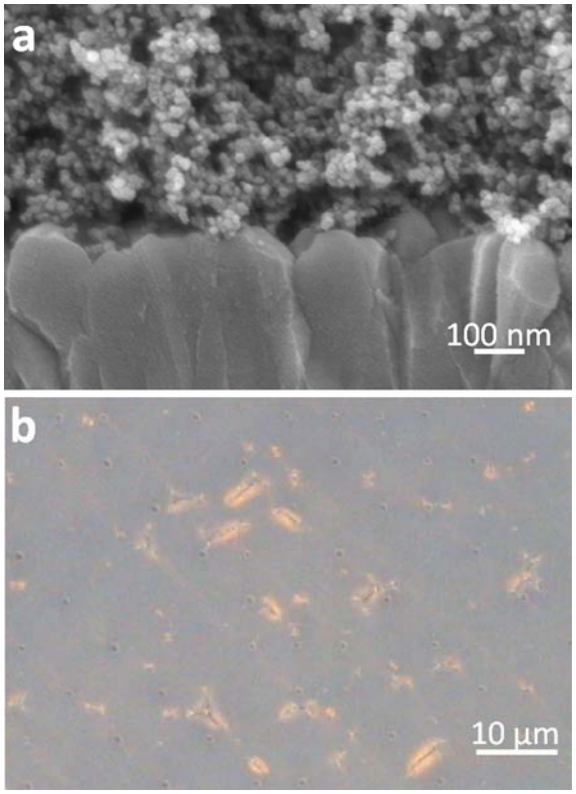

Figure 14: a) SEM cross section of a TCO / TiO_2 porous photoelectrode interface, the TiO_2 here still contains not fully disaggregated TiO_2 nano-particles, b) polarized light micrograph of screen printed TiO_2 photoelectrode layer after sintering, illumination from front side of the cell through the TCO.

From a critical film thickness on (typically 10 µm) cracks in the TiO_2 layer can occur during drying and due to shrinking of the layer on the more macroscopic scale.

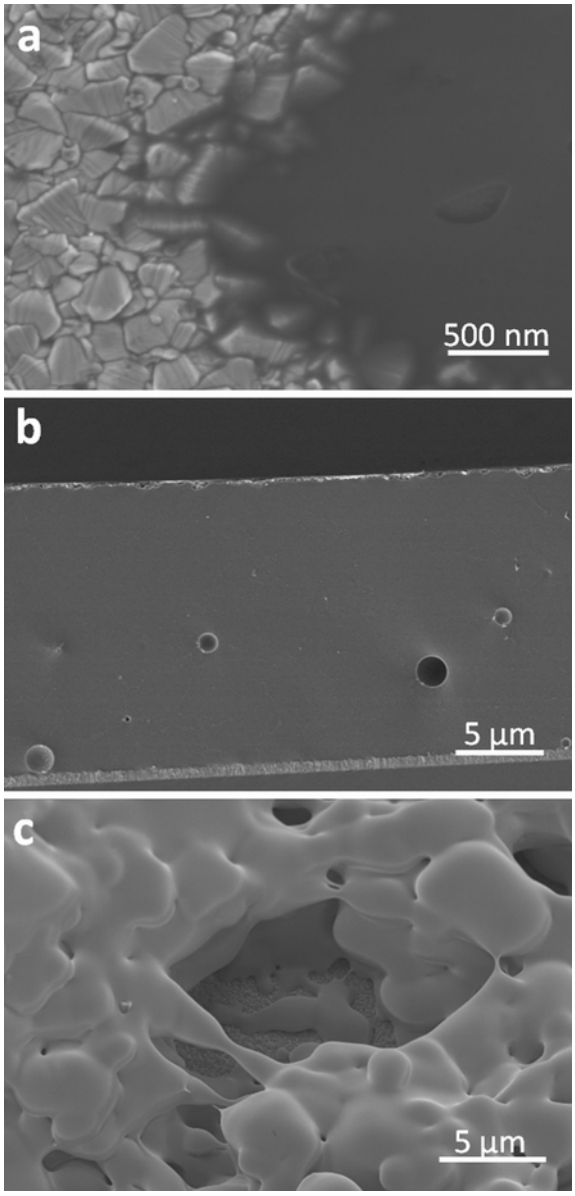

Figure 15: a) SEM top view at the edge of the sintered glass frit layer (right side) showing good wetting of the TCO crystal surface, b) SEM cross section of an improved glass frit layer after sintering on the TCO glass, the layer contains only a few, isolated voids, c) SEM image of extreme void formation in a non-improved glass frit layer during sintering.

As we could observe by polarized light microscopy, the TiO_2 layer is not only vertically damaged by the drying cracks, the whole area of the TiO_2 around the often star like shaped cracks is levelled off from the TCO. This leads to an overall loss of photocurrent. In the microscopic image of figure 14b these areas appear

bright because of an increased reflection of light at the additional formed air – TiO_2 layer interface.
The glass frit needs to generate a very tight, long-term stable external and internal sealing of the module and is therefore determined as one of the critical processes with need for good quality control. Two potential failures in the sealing can be identified; the diffusion of electrolyte species through voids or defects in the glass frit layer or the diffusion or migration of ions through the TCO layer. The quality of the barrier properties at the TCO – glass interface is determined by the wetting properties of the glass frit on the TCO surface. Also scratches or voids inside the TCO layer and between the individual TCO crystals should be filled. We have tested different types of glass frit materials; figure 15a and b show a successful case.

The quality of the glass frit layer is strongly determined by the sintering process of the layer and the particle distribution in the screen print paste. A smooth sintering of the layer results in the homogenous formation of interlinks between the individual glass particles during melting. A high degree of dispersion of particles in the paste seems to be necessary in order to avoid an irregular spacing between the particles which can result in the unwanted entrapment of air (figure 15c).

4 CONCLUSIONS

The up-scalability of dye solar modules to an area of 60 cm x 100 cm on single substrates has been shown for the first time. This has been possible by screen printing a glass frit containing paste followed by sintering and fusing of the substrates in an infrared type furnace without applying mechanical forces. The electrical interconnection at crossing points of the metal finger collector lines has been achieved during the fusing step by making use of a meander type layout. Specific equipment has been developed for the process steps coloration, electrolyte filling and end-sealing.

An analysis of the present module performance and a quality related investigation of the manufacturing have been performed with the aim to promote a near future pilot-production of large scaled dye solar modules.

ACKNOWLEDGEMENTS

This collaborative research has been supported by the BMBF (German Federal Ministry of Education and Research, contract number 03X3519B, project name “FSZ Industrie”), the European commission (contract number 212792, project name “Robust DSC”) and the Ministry for Environment of Baden-Württemberg under contract number BUT011. We would like to thank the partners from the Robust DSC project, especially the company 3GSolar (Israel), for giving valuable input and data on cost estimations, life cycle analysis and energy payback time and for making the LCA-tool available for further calculations [11]. Also, we would like to thank Heinrich Berg from Fraunhofer ISE for performing the hail tests, and, for collaboration on setting up the automated coloring and filling station and for fruitful discussions in lead-user workshops; we would like to thank Harald Widlroither, Matthias Stabe and Frieder Schnabel from Fraunhofer IAO in Stuttgart.

REFERENCES

[1] Sastrawan R, Beier J, Belledin U, Hemming S, Hinsch A, Kern R, Vetter C, Petrat FM, Prodi-Schwab A, Lechner P, Hoffmann W, New interdigital design for large area dye solar modules using a lead-free glass frit sealing, *Progress in Photovoltaics: Research and Applications* 2006; **14:** 697-709

[2] Fukui A. et al., Dye-Sensitized Photovoltaic Module with conversion efficiency of 8.4%, *Appl. Phys. Express* 2009; **2:** 82202-05

[3] Green MA, Emery K, Hishikawa Y, Warta W, Solar cell efficiency tables (version 36), *Progress in Photovoltaics: Research and Applications* 2010; **18**: 346-352

[4] Harikisun R, Desilvestro H, Long-term stability of dye solar cells, *Solar Energy* 2011; **85**: 1179-1188

[5] Hinsch A, Kroon JM, Kern R, Uhlendorf I, Holzbock J, Meyer A, Ferber J, Long-term stability of dye-sensitised solar cells, *Progress in Photovoltaics: Research and Applications* 2001; **9:** 425-438

[6] Hinsch A, Behrens S, Berginc M, Bönnemann H, Brandt H, Drewitz A, Einsele F, Faßler D, Gerhard D, Gores H, Haag R, Herzig T, Himmler S, Khelashvili G, Koch D, Nazmutdinova G, Opara-Krasovec U, Putyra P, Rau U, Sastrawan R, Schauer T, Schreiner C, Sensfuss S, Siegers C, Skupien K, Wachter P, Walter J, Wasserscheid P, Würfel U, Zistler M, Material development for dye solar modules; results from an integrated approach, *Progress in Photovoltaics: Research and Applications* 2008, **16:** 489-501

[7] Kroon JM, Bakker NJ, Smit HJP, Liska P, Thampi KR, Wang P, Zakeeruddin SM, Grätzel M, Hinsch A, Hore S, Würfel U, Sastrawan R, Durrant JR, Palomares E, Pettersson H, Gruszecki T, Walter J, Skupien K, Tulloch GE, Nanocrystalline dye-sensitized solar cells having maximum performance, *Progress in Photovoltaics: Research and Applications* 2007; **15:** 1-18

[8] Hinsch A, Brandt H, Veurman W, Hemming S, Nittel M, Würfel U, Putyra P, Stabe M, Beucker S, Fichter K, “Dye solar modules for façade applications: recent results from project ColorSol”, *Solar Energy Materials & Solar Cells* 2009; **93:** 820-824.

[9] Hagfeldt A, Boschloo G, Sun L, Kloo L, Pettersson H, Dye-sensitized solar cells, *Chem. Rev.* 2010; **110:** 6595-6663

[10] Kroon J, Brandt H, Breen B, Clifford J, Durrant J, Feigenson M, Jensen K, Forneli A, Goldstein J, Graetzel M, Gruszecki T, Hinsch A, Logunov S, Martinez E, O’Regan B, Palomares E, Petterson H, Prassas M, Sauvage F, Sommeling P, Spratt M, Tabo K, Thampi R, Torres T, Vallon S, Veurman W, Yakupov I, Zakeeruddin S, “Robust DSC project final report”, Robust DSC website, 22 April 2011, < http://www.robustdsc.eu/publications>

[11] Breen B, Feigenson M, Goldstein J, Yakupov I, "Life cycle analysis calculator", Energy center Netherlands website, 22 April 2011, <http://www.ecn.nl/lca>

[12] Matsui H, Kenichi O, Takayuki K, Nobuo T, Thermal stability of dye-sensitized solar cells with current collecting grid, *Solar Energy Materials & Solar Cells* 2009; **93:** 1110-1115

[13] Kato N, Takeda Y, Higuchi K, Takeichi A, Sudo E, Tanaka H, Motohiro T, Sano T, Toyoda T, Degradation analysis of dye sensitized solar module after long-term stability test under outdoor working condition, *Solar Energy Materials & Solar Cells* 2009; **93:** 893-897

[14] Leonardi E, Penna S, Brown TM, Di Carlo A, Reale A, Stability of dye sensitized solar cells under light soaking test, *Journal of Non-Crystalline Solids* 2010; **356:** 2049-2052

[15] Kato N, Higuchi K, Tanaka H, Nakajima J, Sano T, Toyoda T, Improvement in long-term stability of dye-sensitized solar cell for outdoor use, *Solar Energy Materialis and Solar Cells* 2011; **95:** 301-305

[16] Sastrawan R, Photovoltaic modules of dye solar cells, *Dissertation, University Freiburg, Germany, available online*, 2006, pp. 77-122

[17] Gao F, Wang Y, Shi D, Zhang J, Wang M, Jing X, Humphry-Baker R, Wang P, Zakeeruddin S, Grätzel M, Enhance the Optical Absorptivity of Nanocrystalline TiO2 Film with High Molar Extinction Coefficient Ruthenium Sensitizers for High Performance Dye-Sensitized Solar Cells, *Journal of the American Chemical Society,* 2008; **130** (32): 10720-10728

[18] Würfel U, Peters M, Hinsch A, Detailed Experimental and Theoretical Investigation of the Electron Transport in a Dye Solar Cell by Means of a Three-Electrode Configuration, *J. Phys. Chem. C* 2008, **112**: 1711-1720

[19] Han L, Koide N, Chiba Y, Islam A, Mitate T, Modeling of an equivalent circuit for dye-sensitized solar cells: improvement of efficiency of dye-sensitized solar cells by reducing internal resistance, *Comptes Rendus Chimie* 2006; **9**: 645-651

[20] Skupien S, Putyra P, Walter J., Kozlowski R, Khelashvili G, Hinsch A, Würfel U, Catalytic materials manufactured by the polyol process for monolithic dye-sensitized solar cells, *Progress in Photovoltaics: Research and Applications* 2009, **17:** 67-73